Compressed liquid speed of sound measurements of cis-1,3,3,3-tetrafluoroprop-1-ene (R1234ze(Z))

Compressed Liquid Speed of Sound Measurements of *cis*-1,3,3,3-tetrafluoroprop-1-ene (R1234ze(Z))

S. Lago[a], P. A. Giuliano Albo[a], J. Steven Brown[b]

[a] *Istituto Nazionale di Ricerca Metrologica, Strada delle Cacce 91, 10135 Torino, Italy*
[b] *Department of Mechanical Engineering, The Catholic University of America, 620 Michigan Ave., NE, Washington, DC 20064, USA*

Abstract

In this paper, 38 speed of sound measurements in the compressed liquid phase of a high purity sample of the novel alternative working fluid *cis*-1,3,3,3–tetrafluoroprop-1-ene (R-1234ze(Z)) are reported along five isotherms, ranging from 273.15 K to 333.15 K for pressures up to 25 MPa. The experimental technique is based on a *double pulse-echo* method resulting in an expanded uncertainty less than 0.05% at the 95% confidence level over the entire thermodynamic space.

Keywords: compressed liquid, high pressure, R1234ze(Z), speed of sound

1. Introduction

Over the last 10 or so years, there has been increased interest in low Global Warming Potential (low-GWP) working fluids as propellants, solvents, foam blowing agents, refrigerants, and in high-temperature heat pumping applications and Organic Rankine Cycle (ORC) applications. This interest has been driven by regulations, legislation, taxing schemes, and a change in public perception. One family of working fluids that has received considerable interest and focus are halogenated olefins, particularly, fluorinated propene isomers (see, e.g., Brown, 2009a; Brown *et al.*, 2010; and other similar example papers too numerous to mention here.) One fluorinated propene isomer possessing a normal boiling point temperature appropriate for high-temperature heat pumping applications and low-temperature Organic Rankine Cycle applications is *cis*-1,3,3,3–tetrafluoroprop-1-ene, also indicated as R1234ze(Z), (see, e.g., Brown *et al.*, 2009). Akasaka *et. al.* (2014) developed a high-accuracy fundamental Equation of State (EoS) for R1234ze(Z) valid for pressures less than 6 MPa, based on experimental values of vapour pressures, saturated liquid and vapor densities, *pvT* data in the liquid and vapor phases, and vapor phase sound speeds. The reader is referred to Akasaka *et. al.* (2014) for references to the papers which report the above mentioned experimental measurements. To the best of the authors' knowledge, there are no experimental speed of sound measurements in the compressed liquid phase of R1234ze(Z) that have been reported in the publicly available literature. Therefore, this paper wishes to contribute to the characterization of R1234ze(Z) by reporting speed of sound measurements in the compressed liquid phase. The hope is that these data will prove useful for developing more refined and accurate formulations of EoS for R1234ze(Z),

*Phone: +39.011.3919.628 Fax: +39.011.3919.621
Email address: s.lago@inrim.it (S. Lago)

which will assist researchers and industry in further developing this alternative low-GWP working fluid.

2. Experimental section

The test sample of *cis*-1,3,3,3-tetrafluoroprop-1-ene (R1234ze(Z), $CF_3CH = CHF$; CAS number 29118-25-0) was provided by Central Glass Co., Ltd. with a declared purity greater than 0.99 in mass fraction. Since the effects of impurities of this order of magnitude on speed of sound measurements are negligible when compared to other sources of uncertainties, no further analysis or purification were attempted on the sample.

2.1. Principle and apparatus for speed of sound measurements

In the present work, compressed liquid speed of sound measurements were taken by employing an advanced transient technique, in particular the double *pulse-echo* technique (Trusler 1991). This method is based on the determination of the time needed by an acoustic wave packet to travel a known distance in a fluid sample. In particular, an electric tone-burst is used to excite a piezoelectric (PZT) source generating two ultrasonic signals which propagate in opposite directions while spreading into the sample, which is maintained at a fixed thermodynamic state. The electrical signal has the form of a five cycles repeated tone-burst with an amplitude of 10 V_{pp}. A detailed description of the complete apparatus, and of the experimental technique, can be found in Lago *et al.* (2006).

The experimental apparatus was an improved version of the system described previously in Benedetto *et al.* (2005) and in Giuliano Albo *et. al.* (2014). In particular, for measurements made in a compressed liquid (therefore with sound speeds typically below 1000 $m \cdot s^{-1}$), it is of fundamental importance to carefully choose the dimensions of the sensor. In this work, the sensor was constructed from 316L stainless steel with two spacer tubes with nominal lengths of 67 mm and 45 mm, with inside and outside diameters of 25 mm and 33 mm, respectively (see Figure 1). Acoustic path lengths were chosen in combination with the source diameter of 7 mm and the tone-burst carrier frequency of 4 MHz. Using this combination, *near-field* effects are avoided and time-of-flight measurements are independent from the chosen frequency up to 5 MHz. By using 4 MHz, it is possible to measure speeds of sound down to 500 $m \cdot s^{-1}$. Furthermore, the chosen lengths represent an acceptable trade-off between shorter distances, which reduce wave damping and accuracy, and longer trajectories, which increase wave damping and accuracy. Shorter cells are not recommended for measurements in compressed liquids because, depending on the source diameter, it is possible to fall into geometrical configurations in which wrong, but repeatable, time-of-flight evaluations are possible. The acoustic path length difference of the cell was determined in ambient conditions by calibration with degassed Millipore ultra-quality water at $T = 298.15$ K and $p = 0.1$ MPa against the speed of sound given by the 1995 EoS formulation of the International Association for the Properties of Water and Steam (IAPWS-95) which, for this particular state point, has an uncertainty of 0.005% as declared in Wagner and Pruss (2002), according to the procedure described in Lago *et al.* (2006).

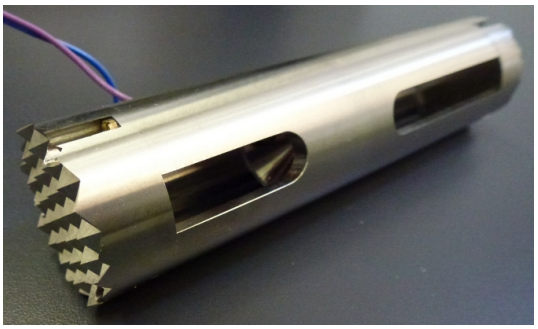

Figure 1: Sensor used for speed of sound measurements in compressed liquids. Different path lengths are revealed by the asymmetry of the loops. Pyramids, on the outer surfaces of the reflectors, prevent the transmitted signal to return to the receiver, interfering with the main signal.

3. Experimental results

Speed of sound, $w_{\rm exp}$, measurements of R1234ze(Z) in the compressed liquid state were taken for five isotherms (273.15 K, 283.15 K, 293.15 K, 313.15 K, 333.15 K) and for seven different pressures (0.1 MPa, 1.0 MPa, 5.0 MPa, 10.0 MPa, 15.0 MPa, 20.0 MPa, 25.0 MPa).

Since the experimental pressures can differ from the desired values up to about ± 0.15 MPa, in order to be able to produce a regular grid of speed of sound data, the experimental results have been fitted using the following bi-dimensional polynomial

$$w(p,T) = \sum_{i=0}^{M} \sum_{j=0}^{N} a_{ij} (p - p_0)^i (T - T_0)^j \ , \tag{1}$$

where a_{ij} are experimentally determined coefficients, and p_0 and T_0 are reference pressure and temperature values, respectively. The "realigned" values are calculated in order to have them match the desired thermodynamic state points. The degree of the bi-dimensional polynomial, $M = 3$ and $N = 4$, has been chosen so that the differences between the experimental values and those calculated using eq. 1 are less than 10% of the experimental uncertainty in the speed of sound measurements. Table 1 provides the experimental speed of sound, $w_{\rm exp}$, measurements together with the corresponding thermodynamic state points determined by the measured temperature and pressure values. Table 2 lists speed of sound data on the regular mesh obtained by eq. 1, while Table 3 reports the matrix of experimentally determined coefficients, a_{ij} (see Eq. (1)).

Figures 2 and 3 show the compressed liquid speed of sound measurements of R1234ze(Z) as a function of pressure and temperature, respectively. The behavior of the experimental results as shown in Figures 2 and 3 are typical of refrigerants previously measured by the authors and show consistent and expected functional forms, confirming the validity and accuracy of the measurements. To the best of the authors' knowledge there are no other experimental data available in the public literature for compressed liquid speeds of sound of R1234ze(Z). Akasaka *et al.* (2014) developed a high-accuracy fundamental EoS for R1234ze(Z) for pressures less than 6 MPa based on experimental values of

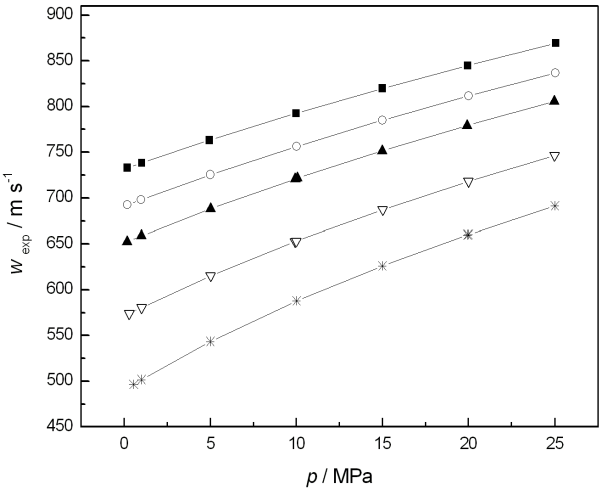

Figure 2: Experimental speed of sound measurements as a function of pressure in R1234ze(Z). Symbols show values for each isotherm: (■), T = 273.15 K; (○), T = 283.15 K; (▲), T = 293.15 K; (▽), T = 313.15 K; (∗), T = 333.15 K.

vapor pressures, saturated liquid and vapor densities, pvT data in the liquid and vapor phases, and vapor phase sound speeds. While not developed from compressed liquid speed of sound data, Akasaka's EoS also could be used to estimate these values. If this is carried out for the experimental results reported in Table 1, the deviations of the measured data from Akasaka's EoS estimates vary from being 1.3% to 7.0% greater, with a mean of 4.1%. While these deviations are significant, they are considered to be acceptable since the EoS was developed without access to this type of data and the fact that compressed liquid speed of sound data are generally sensitive. Thus, the authors recommend that Akasaka's EoS be updated using the experimental compressed liquid speed of sound data reported herein.

4. Assessement of measurement uncertainty

From a metrological point of view, the double *pulse-echo* technique for sound speed determination, as described above, is an indirect measurement method represented by the following model:

$$w_{\mathrm{exp}} = w(\Delta L, \tau, T, p) = \frac{2\Delta L}{\tau_{\mathrm{exp}}} \tag{2}$$

where ΔL, the difference in acoustic path lengths, and τ_{exp}, the measured time of flight, are independent measurements, and temperature T and pressure p are measured state variables. Applying a standard uncertainty propagation

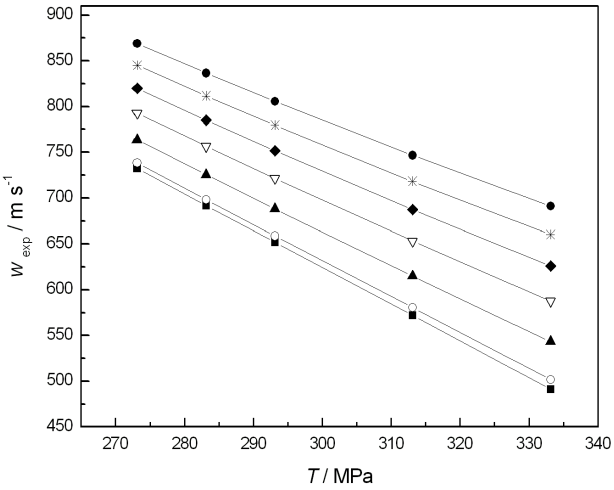

;

Figure 3: Experimental speed of sound measurements as a function of temperature in R1234ze(Z). Symbols show values for each isobar: (■), p = 0.1 MPa; (○), p = 1.0 MPa; (▲), p = 5.0 MPa; (▽), p = 10.0 MPa; (♦), p = 15.0 MPa; (∗), p = 20.0 MPa; (●), p = 25.0 MPa.

procedure to Eq. (2), the following expression for $u(w_{\rm exp})/w_{\rm exp}$ is obtained:

$$\left[\frac{u(w_{\rm exp})}{w_{\rm exp}}\right]^2 = \left[\frac{u(\Delta L)}{\Delta L}\right]^2 + \left[\frac{u(\tau)}{\tau}\right]^2 + \left[\frac{T}{w_{\rm exp}}\left(\frac{\partial w}{\partial T}\right)_p \frac{u(T)}{T}\right]^2 + \left[\frac{p}{w_{\rm exp}}\left(\frac{\partial w}{\partial p}\right)_T \frac{u(p)}{p}\right]^2 . \quad (3)$$

Table 4 lists the contributions to the overall uncertainty from the measured quantities of Eq. (3). As can be seen, the largest contribution comes from the pressure determination while that of temporal delay and repeatability can be considered negligible. The uncertainty contribution due to the temperature measurement is approximately 50% higher then ones measured in liquid hydrocarbons, such as n-alkanes, because of the smaller value of the speed of sound in R1234ze(Z), despite the fact that, $(\partial w/\partial T)_p$ is almost the same for both fluids.

5. Conclusions

In this work, we report 38 compressed liquid speed of sound measurements and their associated uncertainties for a novel alternative working fluid, R1234ze(Z) (*cis*-1,3,3,3–tetrafluoroprop-1-ene), by means of a *double pulse-echo* technique. These results should prove useful for developing more refined and accurate formulations of equations of state for R1234ze(Z), which will assist researchers and industry in further developing this low-GWP working fluid as a propellant, solvent, and foam blowing agent, and for refrigeration, heat pumping, and Organic Rankine Cycle applications.

Reference

Akasaka, R., Higashi, Y., Miyara, A., Koyama, S., 2014. A fundamental equation of state for cis-1,3,3,3-tetrafluoropropene (R-1234ze(Z)). Int. J. Refrigeration 44, 168–176.

Benedetto, G., Gavioso, R.M., Giuliano Albo, P.A., Lago, S., Madonna Ripa, D., Spagnolo, R., 2005. Speed of sound in pure water at temperatures between 274 and 394 K and pressure up to 90 MPa, Int. J. Thermophysics 26 (6), 1667–1680.

Brown, J.S., 2009a. HFO's: New, low global warming potential refrigerants. ASHRAE Journal 51, 22-29.

Brown, J.S., Zilio, C., Cavallini, A., 2009b. The fluorinated olefin R-1234ze(Z) as a high-temperature heat pumping refrigerant. International Journal of Refrigeration 32, 1412-1422.

Brown, J.S., Zilio, C., Cavallini, A., 2010. Thermodynamic properties of eight fluorinated olefins. International Journal of Refrigeration 33, 235-241.

Giuliano Albo, P.A., Lago, S., Romeo, R., Lorefice, S., 2013. High pressure density and speed of sound measurements in n-undecane and evidence of the effects of *near-field* diffraction.

Lago S., Giuliano Albo P. A., Madonna Ripa D., 2006. Speed of sound measurements in n-nonane at temperature between 293.15 and 393 K and pressure up to 100 MPa, Int. J. Thermophys. 27 (4), 1063–1094.

Trusler, J.P.M., 1991. Physical Acoustics and Metrology of Fluids, Taylor & Francis Group., New York.

Wagner, W., Pruss, A., 2002. The IAPSW formulation 1995 for the thermodynamic properties of ordinary water substance for general and scientific use, J. Phys. Chem. Ref. Data 31, 387–535.

R1234ze(Z)		
T_{exp} / K	p_{exp} / MPa	w_{exp} / (m · s^{-1})
273.148	0.192	733.01
273.147	1.017	738.46
273.146	4.940	763.22
273.152	9.982	792.63
273.151	15.012	819.86
273.151	19.968	844.97
273.158	25.059	869.25
283.146	0.194	692.40
283.144	0.979	698.01
283.144	5.005	725.37
283.148	10.017	756.50
283.145	15.005	785.05
283.148	20.019	811.73
283.143	25.023	836.72
293.151	0.198	652.56
293.148	1.001	658.82
293.149	5.029	688.26
293.149	10.065	721.69
293.147	9.940	720.93
293.149	15.001	751.59
293.148	19.929	779.17
293.147	24.979	805.49
313.152	0.320	574.19
313.153	1.010	580.61
313.152	5.026	615.30
313.151	9.998	653.18
313.150	9.927	652.68
313.152	15.023	687.34
313.151	20.004	718.15
313.153	24.987	746.57
333.150	0.554	496.55
333.151	1.002	501.61
333.150	4.999	543.43
333.146	10.015	587.78
333.149	15.006	626.08
333.149	20.009	660.13
333.148	19.956	659.78
333.150	25.005	691.19

Table 1: Experimental measurements of the speed of sound, w_{exp}, of R1234ze(Z) as function of temperature, T_{exp}, and pressure, p_{exp}.

p (MPa)	w (m · s^{-1})	p (MPa)	w (m · s^{-1})	p (MPa)	w (m · s^{-1})	p (MPa)	w (m · s^{-1})	p (MPa)	w (m · s^{-1})	p (MPa)	w (m · s^{-1})	p (MPa)	(m
$T = 273.15$ K													
0.1	732.41	1.0	738.33	5.0	763.54	10.0	792.76	15.0	819.82	20.0	845.10	25.0	8
$T = 283.15$ K													
0.1	691.75	1.0	698.15	5.0	725.27	10.0	756.43	15.0	785.04	20.0	811.59	25.0	8
$T = 293.15$ K													
0.1	651.84	1.0	658.77	5.0	688.01	10.0	721.32	15.0	751.60	20.0	779.50	25.0	8
$T = 313.15$ K													
0.1	572.22	1.0	580.51	5.0	614.99	10.0	653.28	15.0	687.26	20.0	718.04	25.0	7
$T = 333.15$ K													
0.1	491.51	1.0	501.68	5.0	543.23	10.0	587.84	15.0	626.10	20.0	659.94	25.0	6

Table 2: R1234ze(Z) speed of sound measurements as a function of temperature, T, and pressure, p, on a regular grid (see Eq. (1)).

	a_{ij} with $N = 3$ ($i = 0, 1, 2, 3$); $M = 4$ ($j = 0, 1, 2, 3, 4$) and $p_0 = 15$ MPa, $T_0 = 298.15$ K				
	$j = 0$	$j = 1$	$j = 2$	$j = 3$	$j = 4$
$i = 0$	735.247	-3.25144	0.00379791	-3.40437·10^{-5}	9.75196·10^{-7}
$i = 1$	5.9522	0.0314215	7.30976·10^{-5}	-2.71137·10^{-7}	1.03969·10^{-8}
$i = 2$	-0.051567	-0.000762512	-3.88632·10^{-6}	-3.51627·10^{-8}	-2.63479·10^{-9}
$i = 3$	0.00094674	2.48165·10^{-5}	6.09387 ·10^{-7}	6.56473 ·10^{-9}	-1.84995·10^{-10}

Table 3: Matrix of coefficients, a_{ij}, of the speed of sound function (see Eq. (1)) for R1234ze(Z).

Uncertainty source		Relative magnitude
determination of the acoustic path	$u(\Delta L)/\Delta L)$	0.012%
determination of temporal delay	$u(\tau)/\tau)$	0.002%
temperature measurements	$\left(\frac{\partial w}{\partial T}\right)\frac{u(T)}{w}$	0.015%
pressure measurements	$\left(\frac{\partial w}{\partial p}\right)\frac{u(p)}{w}$	0.042%
repeatability		0.001%
Estimated Overall Uncertainty		0.046%

Table 4: Uncertainties budget. All uncertainties are reported at a 95 % confidence level.